Journal of Multidisciplinary Healthcare

Dovepress
Taylor & Francis Group

Open Access Full Text Article

ORIGINAL RESEARCH

Development and Validation of a Machine Learning–Based Clinical Model for Predicting Rupture in Ectopic Pregnancy: A Web-Based Nomogram Approach

Xiongying Zhao[1,*], Tianchen Wu[2,*], Simin Zeng[1], Xiaoyun Yuan[1], Xiaoying Liang[1], Hui Yang[3], Lihui Ye[1]

[1]Department of Ultrasound Diagnosis, Panyu Maternal and Child Care Service Centre of Guangzhou, Guangzhou, Guangdong, 511495, People's Republic of China; [2]Department of Neurology, Nanjing Hospital of Chinese Medicine, Nanjing, Jiangsu, 210001, People's Republic of China; [3]School of Nursing, Nanjing University of Chinese Medicine, Nanjing, Jiangsu, 210046, People's Republic of China

*These authors contributed equally to this work

Correspondence: Lihui Ye, Department of Ultrasound Diagnosis, Panyu Maternal and Child Care Service Centre of Guangzhou, No. 2 Qinghe East Road, Panyu District, Guangzhou, Guangdong, 511495, People's Republic of China, Tel +862039152303, Email lihui_yel@126.com; Hui Yang, School of Nursing, Nanjing University of Chinese Medicine, No. 138 of Xianlin Road, Qixia District, Nanjing, Jiangsu, 210023, People's Republic of China, Tel +862585811993, Email yanghuiyhcc@163.com

Objective: The aim of this study is to develop a predictive model for rupture-associated bleeding in ectopic pregnancy (EP) and to construct a web-based nomogram to support early clinical intervention in women at elevated risk.

Methods: Clinical data were retrospectively collected from 543 women with EP at Hexian Memorial Affiliated Hospital of Southern Medical University, Guangzhou, China, between June 2019 and June 2022. Among these, 58 cases were confirmed intraoperatively to have experienced rupture with bleeding. The cohort was randomly divided into training (70%) and validation (30%) subsets. Key predictive variables were selected using the Extreme Gradient Boosting (XGBoost) algorithm, guided by SHapley Additive exPlanations (SHAP) values. Model performance was assessed using the area under the receiver operating characteristic (ROC) curve, calibration analysis, decision curve analysis (DCA), and clinical impact curve (CIC). A web-based nomogram was subsequently developed for clinical implementation.

Results: Seven predictive variables were identified and used to construct the model. The ROC curve yielded an area under the curve (AUC) of 0.941 (95% CI: 0.882–0.968) in the training subset and 0.970 (95% CI: 0.9405–0.990) in the validation subset. Calibration curves demonstrated strong concordance between predicted probabilities and observed outcomes. DCA indicated a clinically meaningful predictive probability range between 1% and 94.82%. A dynamic, web-based nomogram was created to facilitate practical application.

Conclusion: A clinically applicable predictive model for rupture in EP was developed and validated, incorporating seven key variables. The web-based nomogram enables early risk stratification and intervention, potentially reducing the incidence of rupture-related complications.

Keywords: ectopic pregnancy, machine learning, nomogram, prediction model

Introduction

Ectopic pregnancy (EP) is defined as the implantation of a fertilized blastocyst outside the uterine endometrium. This condition represents approximately 2% of all pregnancies as documented by the Centers for Disease Control and Prevention.[1] The presence of vaginal bleeding or lower abdominal pain during early pregnancy should raise clinical suspicion of EP, with ultrasound examination serving as a critical diagnostic tool.[2] Advances in quantitative beta human chorionic gonadotropin (β-hCG) monitoring and ultrasound imaging have enhanced diagnostic accuracy, contributing to a reduction in EP-related mortality over the past three decades in the United States. Between 2011 and 2013, EP rupture accounted for

Received: 24 April 2025
Accepted: 2 September 2025
Published: 13 September 2025

approximately 2.7% of pregnancy-related mortalities in the US.[3] In lower-resource settings, the mortality associated with ruptured ectopic pregnancy can be alarmingly high due to delayed diagnosis and insufficient medical facilities.[4] Mullany et al discuss the critical role of early diagnosis in preventing serious complications, such as rupture, which leads to severe internal bleeding and may necessitate surgical intervention. They assert that implementing strategies to improve awareness and understanding of EP among healthcare providers can greatly enhance patient safety and improve overall management.[5]

Recent research has systematically identified multiple clinical, laboratory, and imaging factors that correlate with ectopic pregnancy rupture risk. Abdominal pain, as the most common presenting symptom, has been extensively studied as a rupture predictor. Xu et al conducted a comprehensive meta-analysis of 5269 ectopic pregnancy patients and found that 56.4% eventually experienced rupture, with abdominal pain being a significant predictor.[6] Pain characteristics, including severity, location, and timing, have been shown to correlate with rupture probability in large-scale studies. Beyond clinical presentation, serum biomarkers provide objective assessment tools for risk stratification. Progesterone and β-hCG levels have demonstrated well-established predictive value in contemporary research. Abdelfattah-Arafa et al established baseline β-hCG as a predictor of medical treatment failure in tubal ectopic pregnancy, demonstrating that each 1000 IU/L increase was associated with 32% higher odds of failure,[7] which often precedes rupture events. Complementing these laboratory findings, ultrasound imaging features provide direct morphological evidence for rupture risk assessment. Mass location, particularly ampullary implantation, has been identified as a crucial anatomical factor due to differences in tubal distensibility and vascular supply.[6] The importance of mass dimensions was confirmed by Aiob et al, who demonstrated positive correlations between both maximum diameter and vertical diameter and rupture probability in their cohort study.[8] Additionally, mass border characteristics have been recognized as important ultrasound parameters, with irregular borders suggesting compromised tissue integrity and higher rupture potential. Pelvic fluid collections frequently serve as important indicators of bleeding and impending rupture. The presence of pelvic hematocele, rectouterine pouch effusion, pelvic effusion, or ascites reflects varying degrees of intraperitoneal bleeding. Xu et al confirmed that extensive hemoperitoneum was significantly associated with rupture occurrence.[6] While individual risk factors have been extensively validated, comprehensive prediction models integrating multiple variables through systematic selection remain limited. This study addresses this gap by developing a machine learning approach that systematically incorporates established risk factors through rigorous variable selection processes.

Delayed diagnosis represents a significant risk factor for rupture-associated hemorrhage in EP. Clinical history, serial β-hCG measurements, and ultrasound findings are essential components in both diagnosing EP and identifying rupture risk.[9] Variations in regional, economic, and sociocultural contexts—including limited education on early pregnancy and inadequate access to antenatal care—have contributed to delays in diagnosis and treatment across different populations.

In the present study, demographic characteristics, clinical laboratory results, and ultrasound examination findings were collected to develop a predictive model for EP rupture risk using machine learning techniques. The model was presented as a nomogram, which included a web-based dynamic version to facilitate clinical decision-making by allowing healthcare providers to estimate rupture risk using mobile devices.

Materials and Methods

Study Design and Participants

Data were retrospectively collected from women diagnosed with EP who underwent early pregnancy assessments at Hexian Memorial Affiliated Hospital of Southern Medical University over a three-year period (June 2019 to June 2022/ February 2023). Specific inclusion and exclusion criteria were applied.

Rupture Definition: Tubal rupture was defined as direct visualization of tubal wall disruption with hemoperitoneum during surgical intervention, confirmed by operative findings. In cases managed non-surgically, rupture was defined by the presence of significant free fluid (>100mL) with echogenic debris on ultrasound combined with hemodynamic instability requiring immediate intervention.

The inclusion criteria encompassed the following: (1) women evaluated and diagnosed with pregnancy of unknown location (PUL), those presenting with pregnancy without evidence of intrauterine gestation, or those with confirmed

extrauterine pregnancy; and (2) Clinical presentation consistent with tubal rupture as defined above, confirmed by surgical findings or composite clinical-imaging criteria.

Exclusion criteria were: (1) women with ultrasound findings confirming intrauterine gestational contents or EP defined by the presence of an adnexal mass with an embryonic pole or fetal cardiac activity; and (2) women diagnosed with cesarean scar pregnancy (CSP), a specific EP subtype characterized by implantation at the site of a prior cesarean section, which has distinct diagnostic criteria. CSP was excluded because it represents a distinct clinical entity with different pathophysiology, presentation, and management from tubal ectopic pregnancies. This study focused specifically on tubal ectopic pregnancies to develop a rupture prediction model for this most common form of ectopic pregnancy.

A total of 860 women with EP were initially identified, among whom 66 had confirmed rupture with hemorrhage. Following exclusion of 163 cases due to missing observational data or loss to follow-up, and 155 cases, where the pregnant women declined to provide relevant personal information, 543 cases were included in the final analysis, of whom 58 experienced rupture-related bleeding. All participants provided written informed consent, and ethical approval was granted by the hospital's institutional review board (approval number: 2023071307).

Variables were selected in accordance with established EP diagnosis and management guidelines, in conjunction with diagnostic criteria for ultrasound assessment of EP.[10–12] Blood test results obtained on the day of the B-ultrasound examination were retrieved through the hospital's electronic medical record system. Laboratory and imaging indicators included serum β-hCG, progesterone levels, and ultrasound data obtained using both transabdominal and transvaginal color Doppler ultrasound, the latter utilizing high-resolution transvaginal scanning (TVS).

The following ultrasound and clinical indicators were recorded: endometrial thickness (measured as the maximum anterior-posterior diameter of the endometrial stripe at the fundal level in the sagittal plane during transvaginal ultrasonography, expressed in millimeters); location of mass within the ampulla of the fallopian tube (defined as a mass center > 4 cm from the uterine cornu); the longest and vertical diameters of the mass; the presence of a visible gestational sac (yolk sac-like or embryonic structures within the mass); clarity of mass boundary; presence of pelvic blood clots; uterovesical pouch effusion; rectouterine pouch effusion (anteroposterior diameter > 1 cm); pelvic effusion; ascites; and relevant medical history, including age, weeks of amenorrhea, history of abortion, history of EP, history of pelvic surgery, presence of abdominal pain within one week preceding the ultrasound, and presence of vaginal bleeding. Pelvic effusion was defined as fluid extending beyond the rectouterine pouch, with sonographic evidence of anechoic regions surrounding the uterus and ovaries. Ascites was defined as fluid accumulation in the hepatorenal recess, splenorenal recess, or bilateral iliac fossae.

Ultrasound Examination Protocol

All transvaginal ultrasound examinations were performed by experienced sonographers with minimum 5 years of specialized experience in obstetrical-gynecological ultrasonography. All operators had certification from relevant professional societies. To ensure consistency, all images were reviewed by two senior specialists, and regular calibration sessions were conducted to minimize inter-observer variability.

Statistical Methods

Data analysis was performed using R software (version R-4.2.1) (https://mirrors.tuna.tsinghua.edu.cn/CRAN/) and RStudio (version 2022.07.1 Build 554) (https://www.rstudio.com/about/trademark/). Categorical variables were presented as frequencies and percentages. Normally distributed continuous variables were expressed as mean ± standard deviation (SD), while non-normally distributed variables were summarized as median with interquartile range [M (P25, P75)]. Group comparisons in the baseline table were conducted based on variable type and distribution characteristics. Independent-sample *t*-tests were applied for normally distributed data, the Mann–Whitney *U*-test for non-normally distributed data, and chi-square (χ^2) tests for categorical variables. A two-sided $p < 0.05$ was considered statistically significant. Relevant R packages used in the analysis are detailed in subsequent sections. Data processing and hypothesis testing were conducted through the following steps.

Step 1: Missing value analysis and multiple imputation were performed using the R package (mice). A total of 163 patients with more than 30% missing case information or who were lost to follow-up, along with 155 patients who declined to provide

personal information, were excluded. Consequently, 543 women diagnosed with EP were included in the analysis, of whom 58 experienced EP rupture. Multiple imputation was conducted to minimize bias and enhance model accuracy. The predictive mean matching (pmm) method was applied, generating five imputed datasets (m = 5) with a seed value of 123. Imputed datasets were selected based on the Bayesian Information Criterion (BIC) to ensure optimal model fit.[13]

Step 2: Following multiple imputation, the data were randomly split into training and validation sets at a 7:3 ratio. Three machine learning methods were initially employed for variable screening. After constructing the models, performance was compared using BIC values and receiver operating characteristic (ROC) curves, with DeLong's test applied for significance testing. Given that the importance of variables can vary depending on the machine learning method used, and that evaluation standards are not universally agreed upon, the XGBoost (eXtreme Gradient Boosting) algorithm was selected from the shapviz package. This algorithm iterates based on decision trees to produce a "black box" model. While the XGBoost algorithm typically provides superior prediction accuracy compared to generalized linear models, it has reduced interpretability for linear relationships. To address this, SHAP (Shapley Additive Explanations) values, a widely applicable method, were employed to explain the importance of variables in the model, allowing for a clear understanding of which features most significantly influence the prediction model.[14]

Using SHAP values, the importance of feature variables was ranked to identify the independent variables most influential in affecting the outcome variable. These variables were then compared with those identified through the three previously mentioned machine learning methods to finalize the set of variables included in the prediction model. Among the three methods, LASSO regression analysis, a type of regularized regression analysis, was employed to select variables for model inclusion by adjusting the penalty coefficient.[15] The cutoff point for variable inclusion was typically determined based on the minimum EBIC value or EBIC.1se.[16] In this study, EBIC.1se was selected as the cutoff for the inclusion of independent variables.

After constructing the final prediction model for the risk of EP rupture, a ROC curve was plotted, and Bootstrap validation was conducted with 1000 repetitions to assess model discrimination.[17] The Hosmer-Lemeshow test was applied for calibration testing. Additionally, decision curve analysis (DCA) and the clinical impact curve were utilized to evaluate the model's clinical usability and potential for providing clinical guidance. Finally, a nomogram was developed to visually present the clinical prediction model.[18] The model construction and reporting of results adhered to the TRIPOD statement checklist.[19]

The flowchart outlining the methodology of this study is presented in Figure 1.

Results

Missing Value Analysis and Multiple Imputation

Following multiple imputation of missing values, discrepancies were observed in the fit of the imputed data. Based on the fitting curves of the imputed variables and the BIC, the curve from the fifth imputation exhibited the closest fit. Therefore, the imputed values from iteration 5 were selected to fill the original dataset. The fitting curves for the missing value analysis and multiple imputation are presented in the supplementary materials (Figures S1 and S2).

After performing multiple imputations, the baseline characteristics of the 543 EP patients are presented in Table 1. In the training set (n = 382), there were 342 patients without rupture and 40 patients with rupture. In the validation set (n = 161), 143 patients had no rupture, while 18 had rupture.

Results of Initial Screening and Secondary Screening by Three Machine Learning Models

Results of Univariate and Stepwise Backward Regression Analysis Method

The following 10 variables for further evaluation were identified using univariate regression analysis: abdominal pain, progesterone (PROG), mass in the ampulla of the fallopian tube (Mass (Ampulla)), longest diameter of the mass (Max.Ld), vertical diameter of the mass (Ver.Ld), mass border, pelvic hematocele (PH), rectouterine pouch effusion (RPE), pelvic effusion (PE), and ascites. Stepwise backward regression analysis resulted in the selection of six variables: Mass (Ampulla),

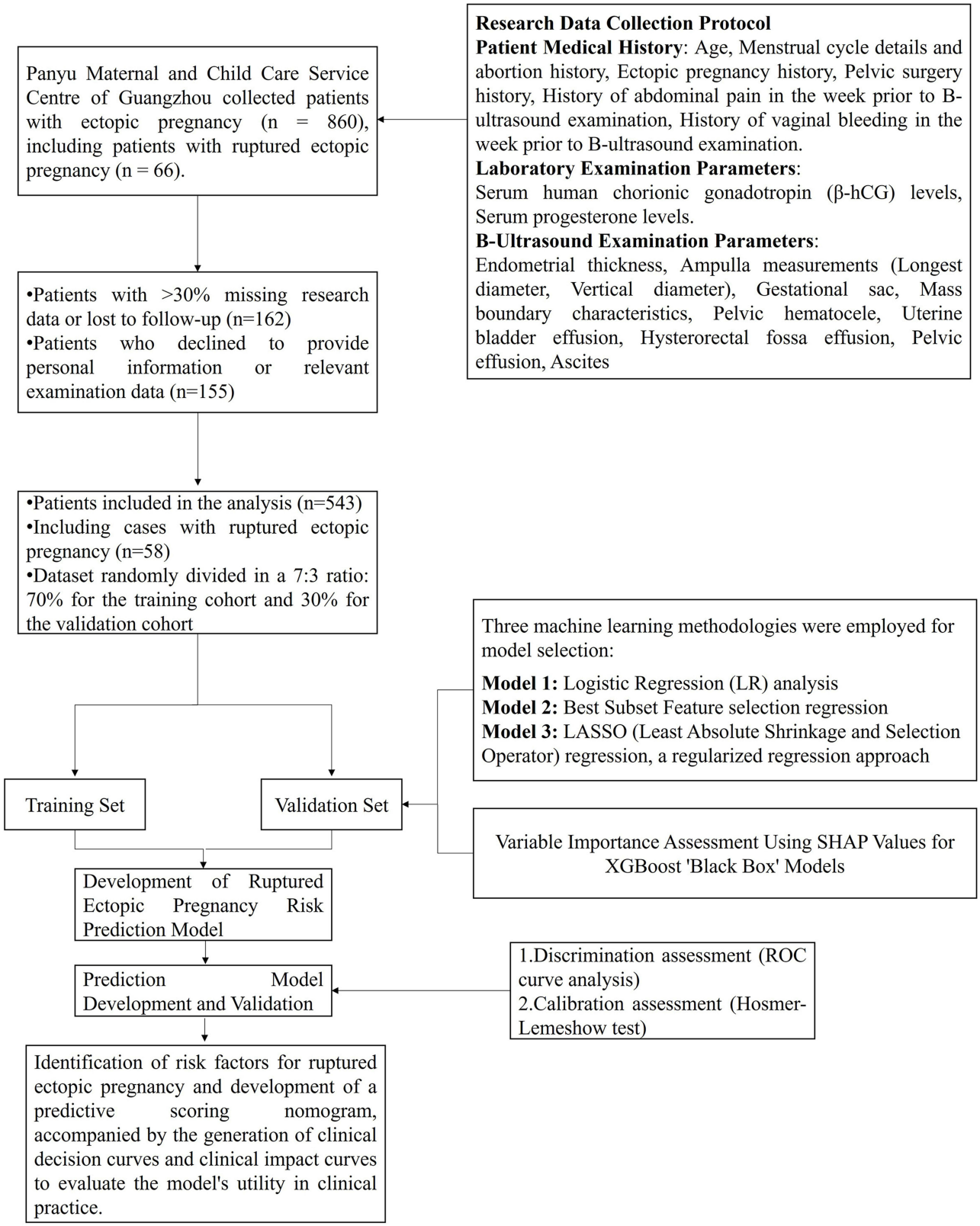

Figure 1 Flowchart of the study selection process.

https://doi.org/10.2147/JMDH.S536476

https://doi.org/10.2147/JMDH.S536476

Table 1 Baseline Characteristics of Subjects Based on Multiple Interpolation

Characteristics	**Training Set (n=382)**			**Validation Set (n=161)**		
Name	No(n=342)	Yes (n=40)	*p*	No (n=143)	Yes (n=18)	*p*
Age [M(P_{25},P_{75}),year]	31.00 (27.00–35.0)	31.50 (27.50 −36.50)	0.527	30.00 (26.50–33.50)	32.50 (30.00–36.0)	0.142
Gestational age [M(P_{25},P_{75}),week]	6.00 (5.00–7.00)	6.00 (5.00–8.00)	0.573	6.00 (5.00 −7.00)	6.00 (5.00–7.00)	0.110
Endometrial thickness [M(P_{25},P_{75}),mm]	10.00 (7.00 −14.00)	7.50 (6.00–11.00)	0.065	10.00 (7.00–14.00)	7.00 (6.00 −10.00)	0.046
History of CS[n(%)]						
No	255 (74.6%)	28 (70%)	0.666	111 (77.6%)	12 (66.7%)	0.376
Yes	87 (25.4%)	12 (30%)		32 (22.4%)	6 (33.3%)	
History of SMM/STOP[n(%)]						
No	154 (45%)	17 (42.5%)	0.892	72 (50.3%)	11 (61.1%)	0.541
Yes	188 (55%)	23 (57.5%)		71 (49.7%)	7 (38.9%)	
History of ectopic pregnancy[n(%)]						
No	287 (83.9%)	38 (95%)	0.104	119 (83.2%)	16 (88.9%)	0.740
Yes	55 (16.1%)	2 (5%)		24 (16.8%)	2 (11.1%)	
History of pelvic surgery [n(%)]						
No	271 (79.2%)	35 (87.5%)	0.304	113 (79%)	14 (77.8%)	0.998
Yes	71 (20.8%)	5 (12.5%)		30 (21%)	4 (22.2%)	
Abdominal pain [n(%)]						
No	109 (31.9%)	4 (10%)	0.007	45 (31.5%)	3 (16.7%)	0.308
Yes	233 (68.1%)	36 (90%)		98 (68.5%)	15 (83.3%)	
Abnormal vaginal bleeding [n(%)]						
No	77 (22.5%)	21 (52.5%)	<0.001	37 (25.9%)	9 (50%)	0.063
Yes	265 (77.5%)	19 (47.5%)		106 (74.1%)	9 (50%)	

β-HCG[M(P_{25},P_{75}),mIu/mL]	2814 (1020 −6998)	5497 (2035–16,042)	0.005	3214 (1246–6656)	7973 (2489–23,644)	0.010
PROG [M(P_{25},P_{75}),ng/mL]	7.12 (3.62–12.89)	3.85 (2.65–7.87)	0.011	7.86 (4.19 13.05)	5.72 (3.25–11.03)	0.217
Mass position[n(%)]						
Left	158 (46.2%)	18 (45%)	0.997	60 (42%)	7 (38.9%)	0.998
Right	184 (53.8%)	22 (55%)		83 (58%)	11 (61.1%)	
Mass (Ampulla)[n(%)]						
No	72 (21.1%)	24 (60%)	<0.001	25 (17.5%)	10 (55.6%)	<0.001
Yes	270 (78.9%)	16 (40%)		118 (82.5%)	8 (44.4%)	
Max. Ld [M(P_{25},P_{75}),cm]	3.10 (2.20–4.50)	6.20 (3.40–8.60)	<0.001	2.80 (2.10–4.05)	7.70 (4.50–9.90)	<0.001
Ver. Ld [M(P_{25},P_{75}),cm]	1.85 (1.50–2.40)	3.30 (2.55–4.60)	<0.001	1.80 (1.40–2.30)	3.90 (2.70–6.20)	<0.001
GS[n(%)]						
No	296 (86.5%)	35 (87.5%)	0.998	120 (83.9%)	16 (88.9%)	0.742
Yes	46 (13.5%)	5 (12.5%)		23 (16.1%)	2 (11.1%)	
Mass border[n(%)]						
Clear	8 (2.3%)	14 (35%)	<0.001	2 (1.4%)	10 (55.6%)	<0.001
Fuzzy	334 (97.7%)	26 (65%)		141 (98.6%)	8 (44.4%)	
PH[n(%)]						
No	241 (70.5%)	15 (37.5%)	<0.001	96 (67.1%)	10 (55.6%)	0.476
Yes	101 (29.5%)	25 (62.5%)		47 (32.9%)	8 (44.4%)	
RPE[n(%)]						
No	152 (44.4%)	8 (20%)	0.005	75 (52.4%)	3 (16.7%)	0.009
Yes	190 (55.6%)	32 (80%)		68 (47.6%)	15 (83.3%)	

(*Continued*)

https://doi.org/10.2147/JMDH.S536476

Table 1 (Continued).

Characteristics	Training Set (n=382)			Validation Set (n=161)		
PE[n(%)]						
No	304 (88.9%)	14 (35%)	<0.001	131 (91.6%)	5 (27.8%)	<0.001
Yes	38 (11.1%)	26 (65%)		12 (8.4%)	13 (72.2%)	
Ascites[n(%)]						
No	324 (94.7%)	15 (37.5%)	<0.001	137 (95.8%)	8 (44.4%)	<0.001
Yes	18 (5.3%)	25 (62.5%)		6 (4.2%)	10 (55.6%)	

Abbreviations: β-HCG, human chorionic gonadotropin; CS, cesarean section; PROG, progesterone; SMM, surgical management of miscarriage; STOP, surgical termination of pregnancy; Mass (Ampulla), mass in the ampulla of the fallopian tube; Max. Ld, Longest diameter of the mass; Ver. Ld, Vertical diameter of the mass; GS, Gestation sac; PH, pelvic hematocele; RPE, rectouterine pouch effusion; PE, Pelvic effusion.

https://doi.org/10.2147/JMDH.S536476

Max.Ld, mass border, RPE, PE, and ascites, as depicted in the forest plot (Figure 2A). Variables identified by univariate analysis are presented in blue, while those selected through stepwise backward regression analysis are demonstrated in red.

Variable Screening Process of LASSO Regression Analysis

The LASSO regression analysis path plot and cross-validation plot are presented in Figure 2B and C. Using lambda.1se as the cutoff point, where log(λ) = −3.35 (indicated by the black dotted line on the X-axis in Figure 2C), six variables with non-zero coefficients were selected: Mass (Ampulla), Max.Ld, mass border, RPE, PE, and ascites. The stepwise backward regression analysis method did not eliminate any variables, so all six factors were retained.

Variable Screening Process Using Optimal Subset Regression Analysis Model Evaluation Criteria

According to the adjusted R^2 ($adjr^2$) model evaluation criterion, the optimal subset regression analysis identified 8 variables: β-HCG, abdominal pain, Mass (Ampulla), Max.Ld, mass border, RPE, PE, and ascites, as presented in Figure 2D. After stepwise backward regression analysis, 7 variables were retained: β-HCG, Mass (Ampulla), Max.Ld, mass border, RPE, PE, and ascites.

Through the three machine learning algorithms described, six variables (Model A) and seven variables (Model B) were identified, with the primary difference between the two models being the inclusion of β-HCG. The AIC values for Model A and Model B were 142.778 and 138.489, respectively. The ROC curves for both models are presented in Figure 3A. Model A achieved an AUC of 0.92 [95% CI (0.860, 0.975)], while Model B achieved an AUC of 0.94 [95% CI (0.891, 0.981)]. Discrimination testing of both models via the DeLong method yielded a Z-value of 1.238 and a *p*-value of 0.2157, indicating no significant difference in discrimination performance between the two models. Based on the SHAP analysis results from the XGBoost model (Figure 3B), variables were ranked according to their contribution to prediction. The analysis revealed that β-HCG had the highest SHAP value, indicating its critical role in the prediction model and supporting its inclusion.

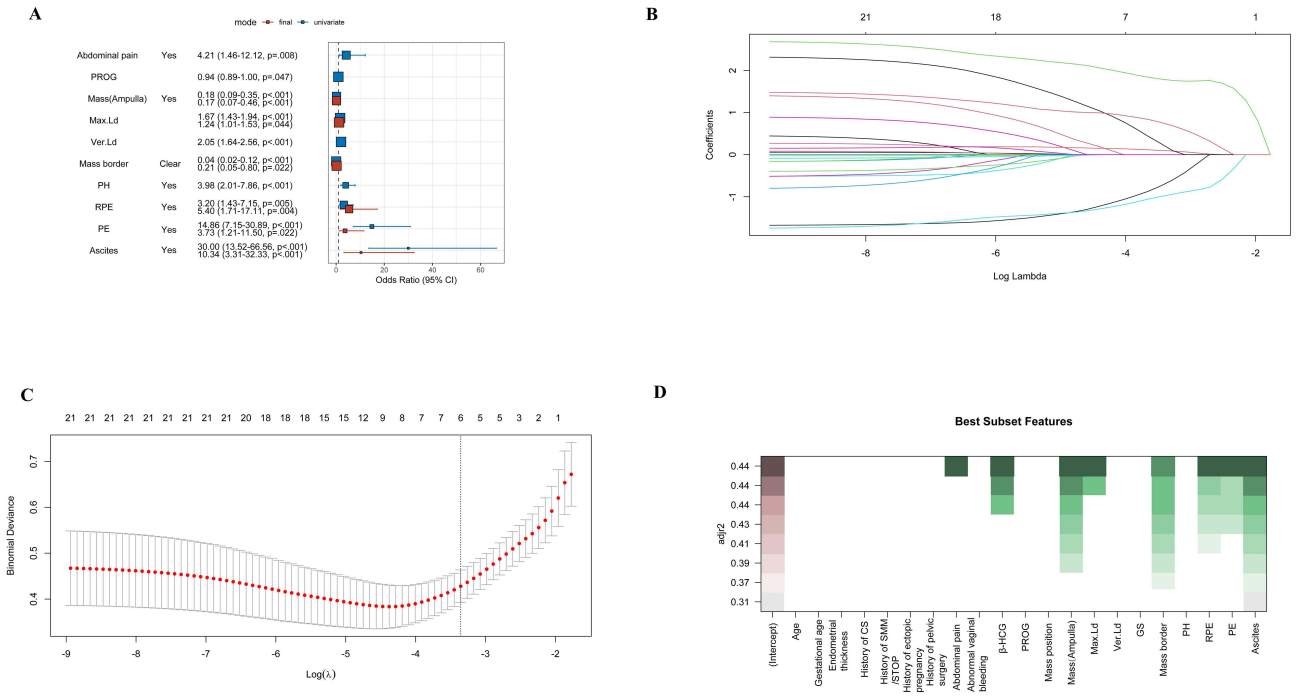

Figure 2 Variable selection process for the rupture prediction model. (**A**) Forest plot displaying odds ratios for selected variables from the stepwise regression analysis. Variables retained in red, excluded in blue. (**B**) LASSO regression coefficient paths illustrating the variable selection process and their coefficients as log(λ) varies. (**C**) Cross-validation plot showing the optimal log(λ) value selected based on minimum error. (**D**) Heatmap representing the best subset features based on their contribution to model performance, showing predictive accuracy across different combinations.

https://doi.org/10.2147/JMDH.S536476

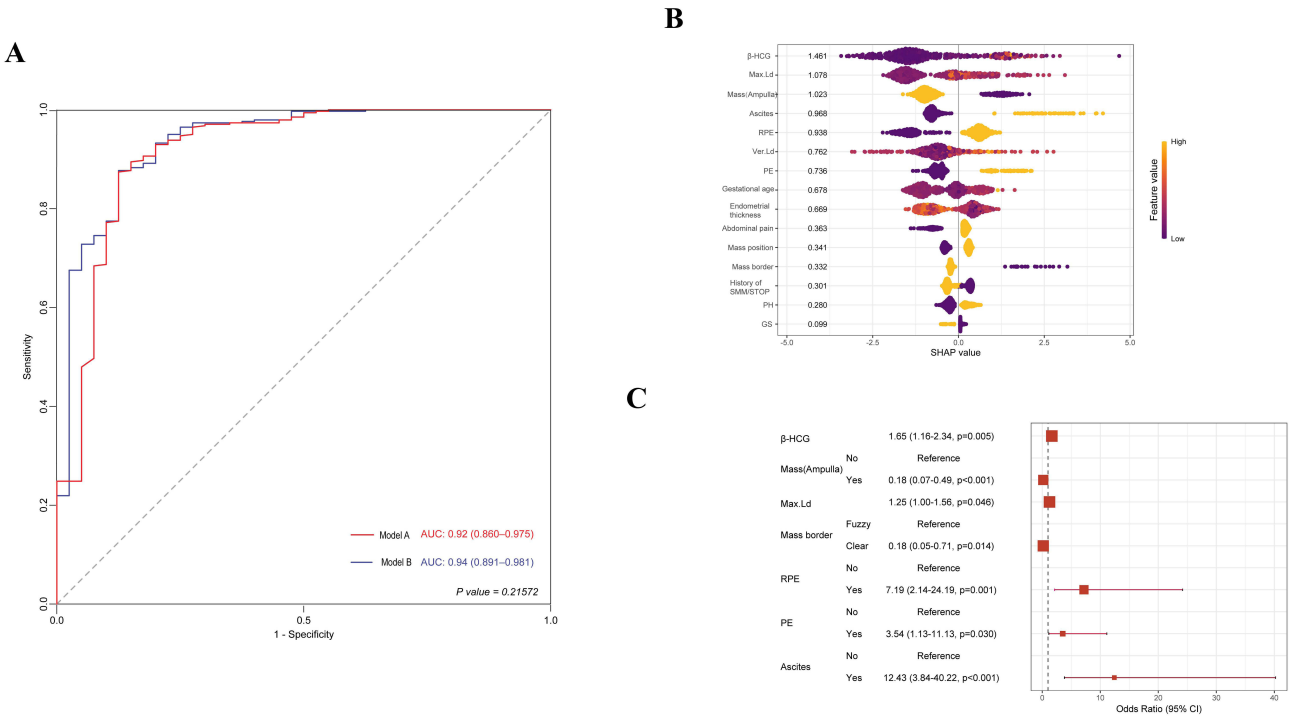

Figure 3 Model performance and predictor significance. (**A**) Receiver Operating Characteristic (ROC) curves for Model A and Model B, with corresponding AUC values. (**B**) SHAP summary plot showcasing the contribution of each variable to the prediction model, indicating variable importance. (**C**) Forest plot displaying adjusted odds ratios and confidence intervals for key predictors identified in the multivariable regression analysis.

Ultimately, combining the machine learning-derived models with clinical interpretability led to the selection of Model B as the final prediction model for EP rupture risk events. The coefficients of Model B are presented in Figure 3C, and the formula for the established model is as follows:

$$L = -3.261 + \beta - HCG * 0.495 - 1.712 * Mass(Ampulla)$$
$$Yes + 0.223 * Max.Ld - 1.696 * Massborder(Clear) + 1.973 *$$
$$\mathrm{RPE(Yes)} + 1.265 * \mathrm{PE(Yes)} + 2.520 * \mathrm{Ascites(Yes)}$$

Results of Prediction Model Discrimination and Calibration Tests

The discrimination of the model constructed in this study underwent Bootstrap validation with n = 1000 repetitions, yielding an area under the ROC curve (AUC) of 0.941 [95% CI (0.882, 0.968)], as presented in Figure 4A. The ROC curve for the validation set also demonstrated an AUC of 0.970 [95% CI (0.9405, 0.990)], as presented in Figure 4B.

The Hosmer-Lemeshow test was performed to assess the calibration of the model in both the training and validation sets. Bootstrap sampling was used to calculate the confidence interval for the Brier Score, with parameters set at 50 samples per repetition, repeated 1000 times (B = 50, M = 1000). The calibration curve for the training set (Figure 5A) indicated a Brier Score of 0.044 [95% CI (0.028, 0.059)], with a Hosmer-Lemeshow test result of $p = 0.053$. The validation set (Figure 5B) demonstrated a Brier Score of 0.034 [95% CI (0.011, 0.059)], with a Hosmer-Lemeshow test result of $p = 0.756$. Both the training and validation sets passed calibration verification, confirming the model's consistency.

Clinical Application and Visual Presentation of the Prediction Model

Based on the constructed prediction model, DCA and Clinical Impact Curve (CIC) were developed for the training set. Both the DCA and CIC indicated that the model provides significant clinical benefits. As presented in Figure 6A, the prediction probability interval for the training set ranged from 1% to 94.82%. Figure 6B presents the red line that represents the number of women assessed as high risk by the model at various probability thresholds, while the blue line

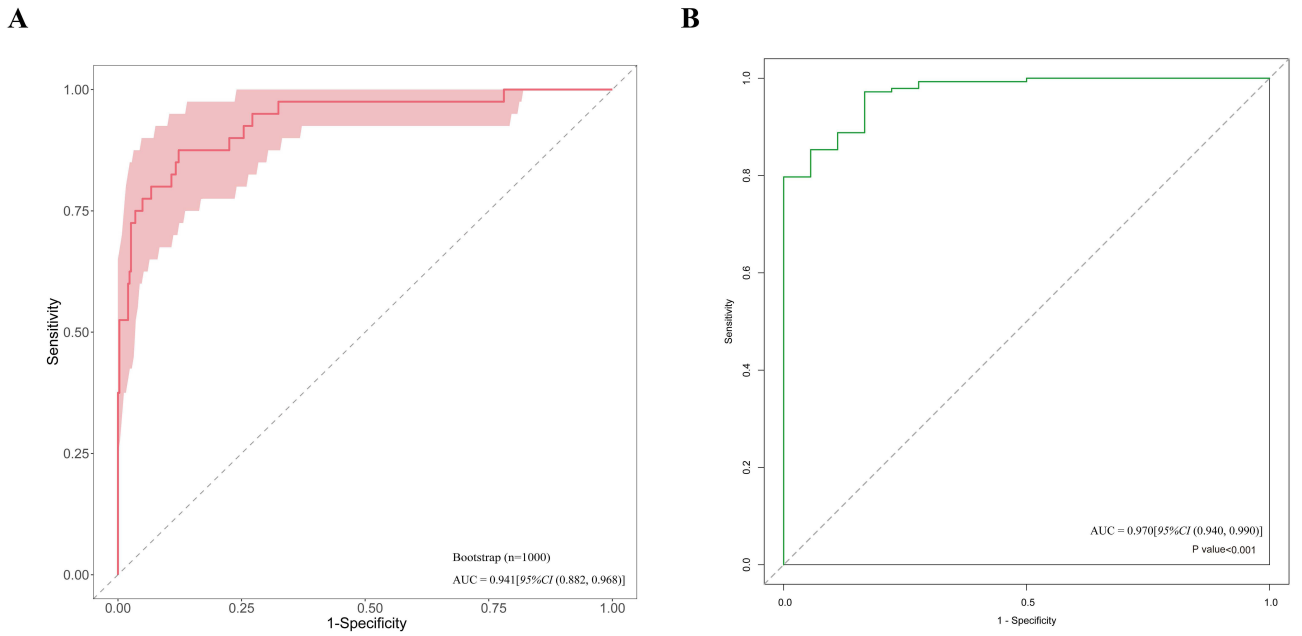

Figure 4 Model validation and performance assessment. (**A**) Bootstrap validation ROC curve (n=1000 iterations) showing model stability with AUC = 0.941 (95% CI: 0.882, 0.968). The shaded area represents confidence intervals from bootstrap resampling. (**B**) External validation ROC curve demonstrating model generalizability with AUC = 0.970 (95% CI: 0.940, 0.990) and statistical significance ($p < 0.001$).

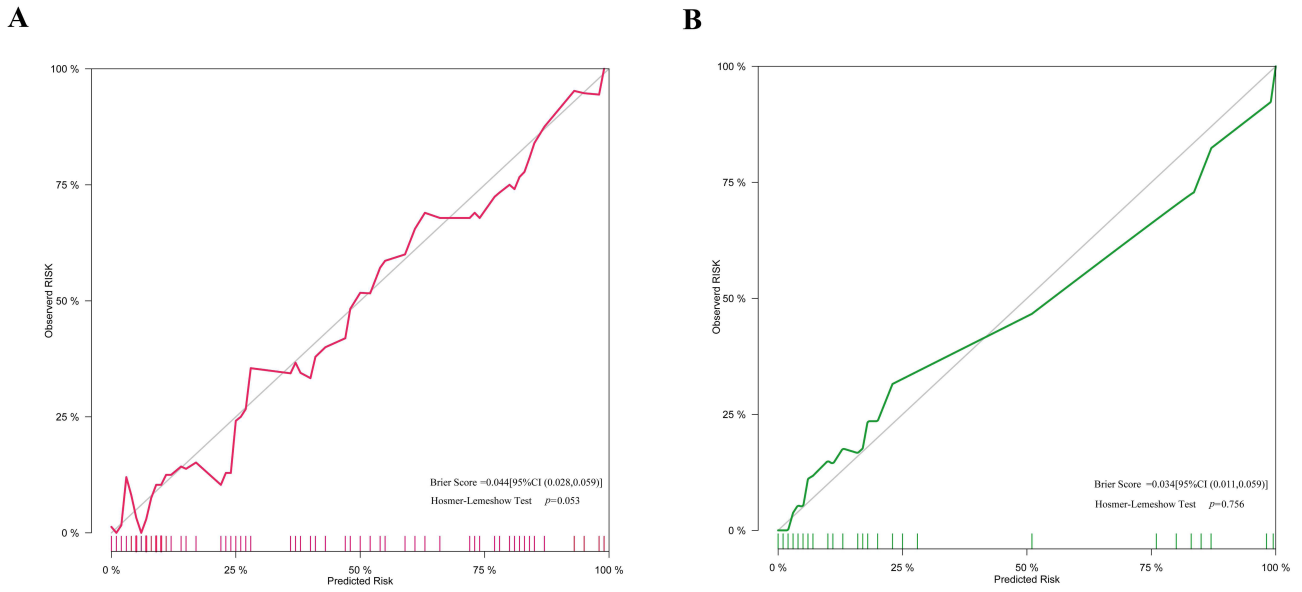

Figure 5 Calibration plots assessing model accuracy. (**A**) Calibration curve for the training set. Brier Score = 0.044; Hosmer-Lemeshow test p = 0.053. (**B**) Calibration curve for the validation set. Brier Score = 0.034; Hosmer-Lemeshow test p = 0.756.

represents the number of high-risk women who actually experienced the outcome event. The relatively parallel red and blue lines indicate that the model has a broad clinical impact threshold. A nomogram was developed for visual representation and clinical application (Figure 7A). To facilitate its use in clinical practice, a web-based nomogram was created using DynNom and the Shiny dynamic nomogram package. The website for the clinical prediction model predicting extrauterine pregnancy rupture is available at https://wutianchen2006.shinyapps.io/DynNomapp_Ectopic_pregnancy_prediction/, as presented in Figure 7B. The example presented in the figure represents a women with β-HCG = 40,000 mIU/mL, EP location in the ampulla of the fallopian tube, a longest mass diameter of 7 cm measured by

https://doi.org/10.2147/JMDH.S536476

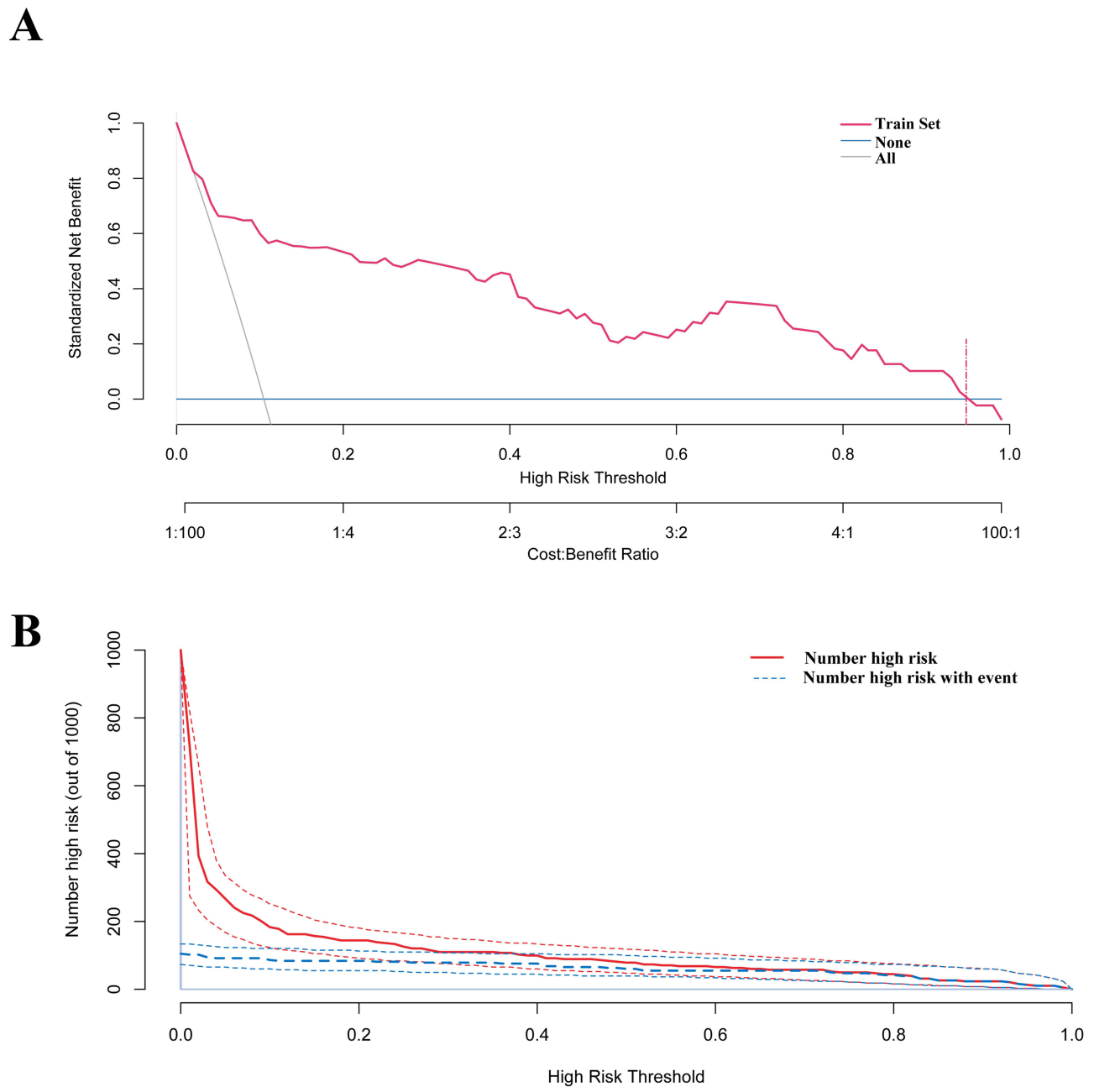

Figure 6 Decision curve analysis and clinical impact assessment. (**A**) Decision curve analysis showing the standardized net benefit of the prediction model across different threshold probabilities, with corresponding cost: benefit ratios. (**B**) Clinical impact curve displaying the number of high-risk patients and those with actual events at various risk thresholds, demonstrating the model's clinical utility.

ultrasound, a clear mass boundary on ultrasound, fluid in the rectouterine pouch and pelvic cavity, and no fluid in the abdominal cavity. The red line and black center point indicate the predicted probability and its confidence interval.

Validation of Ultrasonographic Parameters: Comparison with Surgical Findings

To validate the accuracy of ultrasonographic parameters utilized in our prediction model, we systematically compared preoperative imaging findings with intraoperative surgical observations in all 58 confirmed EP rupture cases. Ultrasonographic measurements revealed mean mass diameter of 43±3 mm, compared to 40±2 mm observed during surgical exploration, with the slight overestimation by ultrasound attributed to the inclusion of surrounding hematoma and blood clots during measurement, which is consistent with expected imaging characteristics in ruptured ectopic pregnancies and

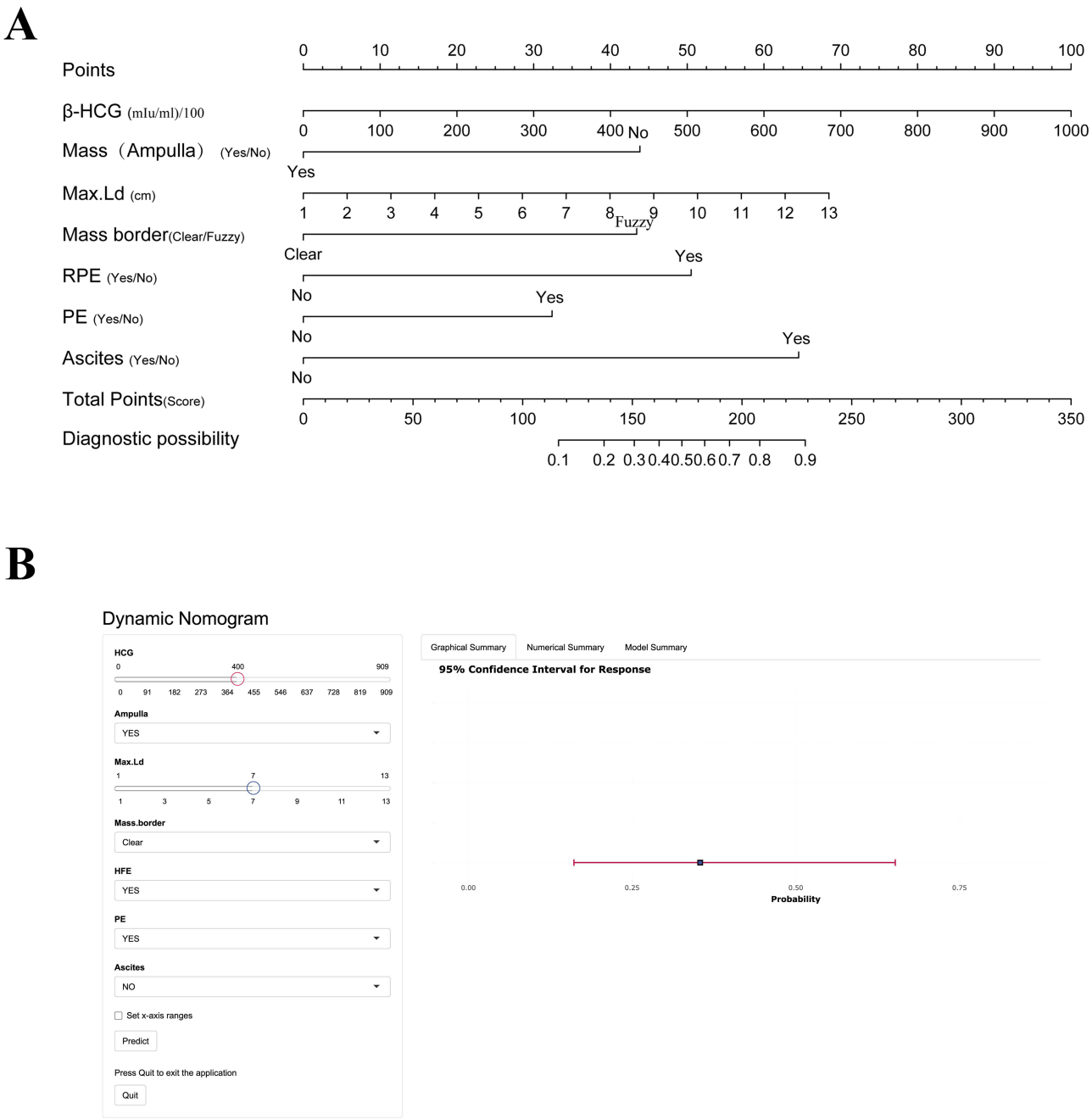

Figure 7 Nomogram for rupture risk prediction in ectopic pregnancy patients. (**A**) Traditional nomogram showing point allocation for each variable and total risk score calculation. (**B**) Dynamic web-based nomogram interface with interactive features for real-time risk assessment. The red and blue circle indicators represent interactive selection buttons for variable input options in the web-based application interface.

demonstrates that ultrasonographic mass measurement provides reliable assessment of ectopic pregnancy size for clinical decision-making. Furthermore, ultrasonographic assessment identified clear borders in 13/58 cases (22.4%) and irregular borders in 45/58 cases (77.6%), with surgical exploration confirming that the majority of ruptured cases indeed presented with compromised tubal integrity, thereby supporting the clinical utility of irregular border appearance as an ultrasonographic predictor of tubal wall disruption and rupture risk. Additionally, ultrasonographic evaluation detected significant intraperitoneal fluid in 43/58 cases (74.1%), with surgical exploration confirming extensive hemoperitoneum in the majority of these cases, although ten cases demonstrated less bleeding than anticipated based on imaging findings, which validated that qualitative assessment of fluid presence in the rectouterine pouch and pelvic cavity serves as a reliable indicator for surgical

https://doi.org/10.2147/JMDH.S536476

decision-making rather than requiring precise volume quantification. Overall, the systematic comparison between ultrasonographic and surgical findings supports the predictive value of the imaging parameters incorporated in our nomogram, with the consistent patterns observed between preoperative ultrasound characteristics and intraoperative findings validating the clinical utility of these parameters for EP rupture risk assessment in clinical practice.

Discussion

This observational study on EP-related events was conducted over a 3-year period at Hexian Memorial Affiliated Hospital of Southern Medical University. Through appropriate data screening and inclusion criteria, missing data were handled using multiple imputation methods. Three machine learning techniques were employed, combined with a "black box model", and SHAP values were used to rank the importance of variables. This process ultimately identified 7 key factors, which were used to construct a clinical prediction model. The model underwent thorough validation through discrimination testing, calibration testing, DCA, and clinical impact curve plotting, with the results displayed as both static and web-based nomograms.

EP has a relatively high incidence among pregnant women worldwide, and delayed treatment of EP rupture can significantly increase the risk of maternal mortality. The use of transvaginal ultrasound and serial β-hCG measurements has been demonstrated to reduce the need for diagnostic laparoscopy in EP cases.[20] Currently, the understanding of EP risk factors and related technologies is well-established. Improvements in medical standards and the widespread adoption of regular prenatal and ultrasound examinations have led to a declining incidence of EP rupture. However, in regions with limited medical resources or in populations without adequate access to prenatal care, the risk of EP rupture remains high, posing serious threats to the health and safety of pregnant women.

The analysis indicated that seven risk factors were associated with the occurrence of EP rupture. These included β-HCG levels, the presence of a mass in the ampulla of the fallopian tube, the Max.Ld, Mass.border, presence of RPE, presence of PE, and presence of ascites as assessed via ultrasound. A cross-sectional study conducted by Darkhaneh et al, which examined 247 cases of tubal EP, reported that elevated β-HCG levels were a significant risk factor for tubal rupture. Patients with β-HCG levels exceeding 1750 IU/mL were more likely to experience rupture.[21] Moreover, Elito Jr. et al found that a β-HCG cut-off value of 2906 IU/mL was associated with stage III invasion in a prospective study of patients with ectopic pregnancy, indicating its relevance in assessing the risk of complications such as rupture.[22] Similarly, Dinc and Issın found that β-hCG levels ≥2799 mIU/mL demonstrated strong predictive value for stage III trophoblastic infiltration with 78.9% sensitivity and 53.8% specificity, indicating increased rupture risk in tubal ectopic pregnancies.[23] This trend may reflect the tendency of patients with β-HCG levels near this threshold to present with early symptoms such as vaginal bleeding and abdominal pain, enabling timely medical intervention.

Therefore, Abdominal pain, vaginal bleeding, and β-HCG levels > 1500 mIU/mL are considered important indicators of potential rupture. In the current analysis, after standardization of β-HCG data, each one standard deviation increase in β-HCG was associated with a 65% increase in rupture risk (OR = 1.65, 95% CI: 1.16–2.34, P = 0.004). Due to variability in gestational age and hormone levels among the study participants at presentation, a specific cut-off value was not established. Instead, the objective was to evaluate the trend between β-HCG levels and rupture occurrence.

The risk of rupture in EP varies depending on the implantation site, particularly whether the pregnancy is located in the ampulla of the fallopian tube. A retrospective observational study conducted by Naimi et al, which included 30,247 pregnancy events at a tertiary hospital over a 10-year period (2008–2018), reported an EP incidence rate of approximately 1.05%.[24] The majority of cases were located within the fallopian tubes, with only 2% occurring in alternative locations such as the ovary.

In a study by Bouyer et al, which examined 1800 surgically treated EP cases from 1992 to 2001, detailed records indicated that approximately 4.5% of EPs were extra-tubal (ovarian or abdominal), while the remainder were primarily tubal.[25] Among these, 73% were located in the ampulla, followed by 2.4% in the interstitial portion, 12.0% in the isthmus, and 11.1% in the fimbria. Non-ampullary tubal and extra-tubal EPs have been associated with a higher risk of morbidity due to rupture-related bleeding.[26,27]

To address diagnostic limitations, the International Society of Ultrasound in Obstetrics and Gynecology (ISUOG) introduced the term "pregnancy of unknown location" (PUL) to describe cases where transvaginal ultrasound (TVS) fails to detect intrauterine or extrauterine gestation or retained products of conception.[28,29] Although not a definitive diagnosis,

the term aids in classifying pregnancies in women with positive pregnancy tests. The ISUOG has also issued quality standards for in-hospital ultrasound to maintain PUL rates below 15%. Patients initially classified as PUL require clinical follow-up to determine final outcomes, which may contribute to reducing mortality associated with undetected EPs, particularly those located in less common implantation sites.

Findings from the present analysis indicated that EP located in the ampulla of the fallopian tube was associated with an 82% reduction in rupture risk compared to non-ampullary locations (OR = 0.18, 95% CI: 0.07–0.49, $p < 0.001$). This indicates that the reduced rupture risk may not be attributable solely to the anatomical characteristics of the ampulla, but rather to the higher detection rate through ultrasound. Early diagnosis and timely intervention in ampullary EPs likely contribute to the observed decrease in rupture incidence.

Current ultrasound-based diagnosis of EP primarily relies on specific grayscale imaging features, including:[30,31] (1) the presence of an inhomogeneous mass adjacent to the ovary or the "speckled sign", which moves independently of the ovary; (2) a mass exhibiting a hyperechoic ring surrounding a gestational sac, referred to as the "concentric circle sign" or "bagel sign"; (3) a gestational sac with detectable cardiac activity, indicative of a viable EP; and (4) a gestational sac containing an embryo without cardiac activity, indicative of a non-viable ectopic pregnancy. Diagnosis of EP should not be based solely on the absence of an intrauterine gestational sac. Instead, confirmation should be based on the positive identification of an adnexal mass through two-dimensional (2-D) grayscale TVS.

A recent study by Mutiso et al investigating the correlation between sonographic and intraoperative findings in ectopic pregnancies emphasized that ultrasound examination forms the cornerstone of EP diagnosis, with specific sonographic features serving as key diagnostic indicators.[32] Specifically, a mass exhibiting a hyperechoic ring or an inhomogeneous adnexal mass with an ill-defined boundary such as the speckled sign were identified as major indicators. Recent evidence by Solangon et al[30] investigating ovarian ectopic pregnancy demonstrated that ultrasound diagnosis can achieve a diagnostic accuracy of 75% on initial examination, with gestational sacs typically presenting well-defined hyperechogenic walls as key sonographic features. Additionally, rupture and associated bleeding in EP may be influenced by the presence of a hyperechoic ring around the gestational sac or adnexal mass, as well as by the size of the ectopic mass, with greater hemorrhage typically associated with larger masses.[33] A systematic review and meta-analysis evaluating early pregnancy ultrasound diagnosis of EP indicated that, across 21 cohort studies involving 2787 women in early pregnancy, the sensitivity of detecting an ectopic mass for predicting potential rupture risk was 63.5%, while specificity reached 91.4%.[34] In the present study, each 1 cm increase in the diameter of the largest cross-sectional area of the ectopic mass detected by ultrasound was associated with a 25% increase in the risk of rupture (OR = 1.25, 95% CI [1.00, 1.56], $p = 0.046$). Additionally, the presence of a clearly defined mass margin was associated with an 82% reduction in rupture risk (OR = 0.18, 95% CI [0.05, 0.71], $p < 0.014$).

Recent retrospective analyses have consistently identified gestational age as a pivotal risk factor for ectopic pregnancy rupture. Goksedef et al demonstrated significantly elevated rupture odds at gestational ages of 6–8 weeks and beyond 8 weeks, with corresponding odds ratios of 3.67 and 46.69 respectively.[35] These findings were corroborated by a comprehensive 10-year cohort study conducted by Sefogah et al,[36] which revealed that each additional week of gestation conferred a 1.69-fold increase in rupture risk, with rupture rates progressively escalating from 47.2% in pregnancies ≤8 weeks to 94.4% in those ≥11 weeks of gestation. Similarly, an observational study conducted in Athens, Greece, between 1988 and 2006 by Sindos et al demonstrated a significant positive correlation between gestational age and the likelihood of rupture.[37] These associations may be attributable to the tendency of ectopic masses to enlarge with increasing gestational age, thereby elevating the risk of rupture. Furthermore, masses with poorly defined margins may reflect underlying abnormalities in tissue architecture, increased vascularization of the surrounding tissue, marked edema, high vessel fragility, and limited tissue extensibility, all of which may contribute to rupture risk.

Contemporary high-resolution transvaginal ultrasonography, particularly three-dimensional imaging combined with color Doppler techniques, enables precise identification and assessment of intraperitoneal hemorrhage and fluid accumulation.[5] The standardized ultrasound evaluation protocols, as recommended by ESHRE[38] and incorporated into international clinical guidelines,[39] demonstrate that both the volume and anatomical distribution of free intraperitoneal fluid are closely correlated with ectopic pregnancy presence and rupture risk assessment. Small amounts of anechoic free fluid in the pouch of Douglas (POD) have been commonly observed in both intrauterine pregnancies and EP, with

approximately 28 to 56% of women with EP presenting with echoic fluid.[40–42] This type of fluid accumulation is frequently physiological. However, when the POD fluid exhibits a "ground glass appearance" and its volume increases alongside gestational progression, particularly when accompanied by symptoms such as abdominal pain, this may indicate intraperitoneal bleeding and should prompt heightened clinical suspicion for EP rupture or imminent rupture.[43]

The presence of blood, as opposed to simple fluid, in the POD warrants further evaluation using an abdominal ultrasound probe to scan the hepatorenal recess (Morrison's pouch). Detection of blood in Morrison's pouch has been considered equivalent to the presence of at least 670 mL of intraperitoneal blood.[44] Winter et al proposed that when substantial volumes of intraperitoneal hemorrhage are detected in women with EP, urgent intervention should be initiated unless alternative diagnoses are confirmed, as EP rupture is strongly associated with elevated mortality.[45]

In the present study, detection of fluid in the POD was associated with a 6.19-fold increase in rupture risk compared to cases without POD fluid (OR = 7.19, 95% CI [2.14, 24.19], $p = 0.001$). The presence of ascites was associated with an even greater increase in rupture risk, with a 11.43-fold elevation compared to its absence (OR = 12.43, 95% CI [3.84, 40.22], $p < 0.001$), indicating a progressively increasing association. For the purposes of this study, pelvic effusion was defined broadly as fluid accumulation in lower pelvic structures, including around the uterus, ovaries, and rectouterine pouch. A study by Liu et al, utilizing computed tomography (CT) to differentiate between ruptured ovarian corpus luteum cyst (ROCLC) and ruptured EP with hemorrhage (REPWH), identified that a mean pelvic effusion depth of 6.96 ± 2.07 cm was indicative of a higher likelihood of rupture in EP.[46] In the current analysis, the presence of pelvic effusion was associated with a 2.54-fold increase in rupture risk compared to cases without effusion (OR = 3.54, 95% CI [1.13, 11.13], $p = 0.030$).

Beyond the final predictors included in our rupture risk model, we retrospectively collected multiple clinical and demographic variables recognized as potential contributors to ectopic pregnancy outcomes, including maternal age, gestational age at presentation, reproductive history (gravidity, parity), prior ectopic pregnancy history, and clinical symptoms (abdominal pain, vaginal bleeding), with variable selection guided by established risk factor literature and clinical guidelines for ectopic pregnancy management.[6,8,47,48] Through systematic feature selection using recursive feature elimination and SHAP value analysis, we identified significant limitations in these variables' predictive utility for rupture risk, finding that maternal age, despite established associations with ectopic pregnancy incidence in epidemiological studies, demonstrated minimal contribution to rupture prediction when integrated with ultrasonographic and biochemical parameters, while reproductive history variables including gravidity, parity, and prior ectopic pregnancy contributed <5% to overall model performance after controlling for objective imaging findings. Clinical symptoms including abdominal pain and vaginal bleeding, while universally important for initial clinical assessment, showed limited discriminatory capacity in our predictive model, with SHAP analysis revealing that symptom-based variables provided marginal additive value beyond objective ultrasonographic and laboratory parameters, achieving only modest independent predictive accuracy. The systematic exclusion of these covariates from our final model reflects adherence to established principles of clinical prediction model development, where parsimony is prioritized to enhance generalizability and prevent overfitting, ensuring that our model focuses on the most discriminative and clinically actionable parameters while maintaining robust predictive performance.

Medical management with methotrexate represents a crucial treatment option for hemodynamically stable patients with unruptured ectopic pregnancies. Our prediction model can guide treatment selection by identifying patients at different rupture risk levels. Patients classified as low-risk (predicted rupture probability <10%) may be considered more suitable candidates for methotrexate therapy, while those with high-risk scores (>30%) might benefit from early surgical consultation and management. Our findings complement recent advances in methotrexate treatment algorithms, such as the scoring system developed by Yeniocak et al,[49] which incorporates similar ultrasonographic parameters including mass size and β-HCG levels for predicting treatment success. While their model focuses on methotrexate success prediction, our rupture risk stratification provides complementary information for clinical decision-making, potentially improving treatment selection and reducing emergency interventions.

This study has several notable strengths and limitations that merit consideration. The primary strengths include: (1) rigorous methodological approach incorporating statistical principles for data selection, missing value analysis, and multiple imputation methods to enhance data completeness and model reliability; (2) comprehensive variable selection

through three complementary machine learning methods combined with SHAP analysis, ensuring the included variables were statistically robust and clinically representative; (3) thorough model validation through multiple performance metrics including ROC analysis, calibration testing, decision curve analysis, and clinical impact curves; (4) practical clinical implementation through both traditional and web-based nomograms, with complete model equations embedded for precise calculations rather than approximate estimates, facilitating convenient patient scoring on mobile devices.

However, several limitations should be acknowledged: (1) the single-center design and predominantly regional patient population may limit generalizability, necessitating external validation across diverse healthcare settings and populations; (2) the retrospective nature of data collection may introduce selection bias and limit the comprehensiveness of clinical variables; (3) focus primarily on conventional ultrasound parameters and standard laboratory indicators may have excluded other potentially relevant biomarkers or advanced imaging features; (4) the relatively small sample size of rupture events (n=58) may affect the stability of model performance estimates; (5) lack of long-term follow-up data to assess the clinical impact of model-guided treatment decisions on patient outcomes. Future research should address these limitations through prospective multicenter validation studies, incorporation of additional predictive variables, and assessment of clinical utility through implementation trials.

Conclusion

This study successfully developed and validated a machine learning-based prediction model for ectopic pregnancy rupture using XGBoost algorithm and SHAP analysis. The model incorporates seven clinically accessible predictors (β-HCG, Mass (Ampulla), Max.L, Mass border, RPE, PE, and Ascites) and demonstrated excellent predictive performance in both training and validation cohorts. The validated prediction model was implemented as a web-based nomogram to assist clinicians in making informed treatment decisions for ectopic pregnancy patients: those identified as high rupture risk may benefit from immediate surgical intervention, while patients with low rupture risk could be considered for tubal-preserving approaches or medical management with methotrexate. This practical tool has potential to optimize individualized treatment strategies and improve maternal outcomes through evidence-based risk assessment in ectopic pregnancy management.

Abbreviations

HCG, human chorionic gonadotropin; CS, cesarean section; PROG, progesterone; SMM, surgical management of miscarriage; STOP, surgical termination of pregnancy; Mass (Ampulla), mass in the ampulla of the fallopian tube; Max. Ld, Longest diameter of the mass; Ver. Ld, Vertical diameter of the mass; GS, Gestation sac; PH, pelvic hematocele; RPE, rectouterine pouch effusion; PE, Pelvic effusion.

Data Sharing Statement

All data generated or analysed during this study are included in this article. The datasets used and analysed during the current study are available from either corresponding author on reasonable request. Data requests may be addressed to Lihui Ye (lihui_yel@126.com) or Hui Yang (yanghuiyhcc@163.com).

Ethics Approval and Consent to Participate

This study was conducted with approval from the Ethics Committee of Panyu Maternal and Child Care Service Centre of Guangzhou (20230711307). This study was conducted in accordance with the declaration of Helsinki. Written informed consent was obtained from all participants.

Acknowledgments

All ultrasonographic examinations and interpretations were conducted by qualified medical professionals with appropriate expertise in gynecological ultrasound and obstetric care to ensure study validity and minimize bias. We would like to acknowledge the hard and dedicated work of all the staff that implemented the intervention and evaluation components of the study.

Funding

Guangdong Yiyang Healthcare Charity Foundation (2023CSZ002), the Natural Science Foundation of the Jiangsu Higher Education Institutions of China (No.24KJB360012), and the Priority Academic Program Development of Jiangsu Higher Education Institutions (YSHL202517).

Disclosure

The authors declare no competing interests in this work.

References

1. Bollig KJ, Friedlander H, Schust DJ. Ectopic pregnancy and lifesaving care. *JAMA*. 2023;329(23):2086–2087. doi:10.1001/jama.2023.7292
2. Frasca DJ, Jarrio CE, Perdue J. Evaluation of acute pelvic pain in women. *Am Fam Physician*. 2023;108(2):175–180.
3. Creanga AA, Syverson C, Seed K, Callaghan WM. Pregnancy-related mortality in the United States, 2011-2013. *Obstet Gynecol*. 2017;130 (2):366–373. doi:10.1097/AOG.0000000000002114
4. Gerema U, Alemayehu T, Chane G, Desta D, Diriba A. Determinants of ectopic pregnancy among pregnant women attending referral hospitals in southwestern part of Oromia regional state, Southwest Ethiopia: a multi-center case control study. *BMC Pregnancy Childbirth*. 2021;21(1):130. doi:10.1186/s12884-021-03618-7
5. Mullany K, Minneci M, Monjazeb R, C. Coiado O. Overview of ectopic pregnancy diagnosis, management, and innovation. *Womens Health*. 2023;19:17455057231160349.
6. Xu C, Mao Z, Tan M, et al. Prevalence and related factors of rupture among cases with ectopic pregnancy; a systematic review and meta-analysis. *Arch Acad Emerg Med*. 2024;12(1):e2. doi:10.22037/aaem.v11i1.2172
7. Abdelfattah-Arafa E, Abdussalam HF, Omar Saad M, El Ansari W. The predictors of successful methotrexate treatment of tubal ectopic pregnancy. *J Obstet Gynaecol*. 2024;44(1):2361456. doi:10.1080/01443615.2024.2361456
8. Aiob A, Yousef H, Abu Shqara R, Mustafa Mikhail S, Odeh M, Lowenstein L. Risk factors and prediction of ectopic pregnancy rupture following methotrexate treatment: a retrospective cohort study. *Eur J Obstet Gynecol Reprod Biol*. 2023;285:181–185. doi:10.1016/j.ejogrb.2023.04.030
9. Lattouf I, Lu C, Pixton S, Reid S, Condous G. Is there a difference in the behaviour and subsequent management of ectopic pregnancies seen at first scan compared to those ectopic pregnancies which commence as pregnancies of unknown location? *Aust N Z J Obstet Gynaecol*. 2016;56 (1):107–112. doi:10.1111/ajo.12434
10. Kirk E, Bottomley C, Bourne T. Diagnosing ectopic pregnancy and current concepts in the management of pregnancy of unknown location. *Hum Reprod Update*. 2014;20(2):250–261. doi:10.1093/humupd/dmt047
11. Po L, Thomas J, Mills K, et al. Guideline No. 414: management of pregnancy of unknown location and tubal and nontubal ectopic pregnancies. *J Obstet Gynaecol Can*. 2021;43(5):614–630e611. doi:10.1016/j.jogc.2021.01.002
12. Scibetta EW, Han CS. Ultrasound in early pregnancy: viability, unknown locations, and ectopic pregnancies. *Obstet Gynecol Clin North Am*. 2019;46(4):783–795. doi:10.1016/j.ogc.2019.07.013
13. Noghrehchi F, Stoklosa J, Penev S, Warton DI. Selecting the model for multiple imputation of missing data: just use an IC! *Stat Med*. 2021;40 (10):2467–2497. doi:10.1002/sim.8915
14. Wang K, Tian J, Zheng C, et al. Interpretable prediction of 3-year all-cause mortality in patients with heart failure caused by coronary heart disease based on machine learning and SHAP. *Comput Biol Med*. 2021;137:104813. doi:10.1016/j.compbiomed.2021.104813
15. Mullah MAS, Hanley JA, Benedetti A. LASSO type penalized spline regression for binary data. *BMC Med Res Methodol*. 2021;21(1):83. doi:10.1186/s12874-021-01234-9
16. Ternes N, Rotolo F, Michiels S. Empirical extensions of the lasso penalty to reduce the false discovery rate in high-dimensional Cox regression models. *Stat Med*. 2016;35(15):2561–2573. doi:10.1002/sim.6927
17. Alba AC, Agoritsas T, Walsh M, et al. Discrimination and calibration of clinical prediction models: users' guides to the medical literature. *JAMA*. 2017;318(14):1377–1384. doi:10.1001/jama.2017.12126
18. Park SY. Nomogram: an analogue tool to deliver digital knowledge. *J Thorac Cardiovasc Surg*. 2018;155(4):1793. doi:10.1016/j.jtcvs.2017.12.107
19. Collins GS, Reitsma JB, Altman DG, Moons KG. Transparent reporting of a multivariable prediction model for individual prognosis or diagnosis (TRIPOD): the TRIPOD statement. *BMJ*. 2015;350:g7594. doi:10.1136/bmj.g7594
20. Hendriks E, Rosenberg R, Prine L. Ectopic pregnancy: diagnosis and management. *Am Fam Physician*. 2020;101(10):599–606.
21. Faraji Darkhaneh R, Asgharnia M, Farahmand Porkar N, Alipoor AA. Predictive value of maternal serum beta-hCG concentration in the ruptured tubal ectopic pregnancy. *Iran J Reprod Med*. 2015;13(2):101–106.
22. Elito J Jr, Ferreira DF, Araujo Junior E, Stavale JN, Camano L. Values of beta-human chorionic gonadotrofin as a risk factor for tubal pregnancy rupture evaluated by histopathology. *J Matern Fetal Neonatal Med*. 2014;27(6):637–639. doi:10.3109/14767058.2013.823940
23. Dinc K, Issin G. Novel marker to predict rupture risk in tubal ectopic pregnancies: the systemic immune-inflammation index. *Ginekol Pol*. 2023;94 (4):320–325. doi:10.5603/GP.a2023.0010
24. Al Naimi A, Moore P, Bruggmann D, Krysa L, Louwen F, Bahlmann F. Ectopic pregnancy: a single-center experience over ten years. *Reprod Biol Endocrinol*. 2021;19(1):79. doi:10.1186/s12958-021-00761-w
25. Bouyer J, Coste J, Fernandez H, Pouly JL, Job-Spira N. Sites of ectopic pregnancy: a 10 year population-based study of 1800 cases. *Hum Reprod*. 2002;17(12):3224–3230. doi:10.1093/humrep/17.12.3224
26. Kang OJ, Koh JH, Yoo JE, et al. Ruptured hemorrhagic ectopic pregnancy implanted in the diaphragm: a rare case report and brief literature review. *Diagnostics*. 2021;11(12):2342. doi:10.3390/diagnostics11122342
27. Gaskins AJ, Missmer SA, Rich-Edwards JW, Williams PL, Souter I, Chavarro JE. Demographic, lifestyle, and reproductive risk factors for ectopic pregnancy. *Fertil Steril*. 2018;110(7):1328–1337. doi:10.1016/j.fertnstert.2018.08.022

28. Barnhart K, van Mello NM, Bourne T, et al. Pregnancy of unknown location: a consensus statement of nomenclature, definitions, and outcome. *Fertil Steril*. 2011;95(3):857–866. doi:10.1016/j.fertnstert.2010.09.006
29. Pellerito J, Bromley B, Allison S, et al. AIUM-ACR-ACOG-SMFM-SRU practice parameter for the performance of standard diagnostic obstetric ultrasound examinations. *J Ultrasound Med*. 2018;37(11):E13–E24. doi:10.1002/jum.14831
30. Solangon SA, Naftalin J, Jurkovic D. Ovarian ectopic pregnancy: clinical characteristics, ultrasound diagnosis and management. *Ultrasound Obstet Gynecol*. 2024;63(6):815–823. doi:10.1002/uog.27549
31. Nadim B, Infante F, Lu C, Sathasivam N, Condous G. Morphological ultrasound types known as 'blob' and 'bagel' signs should be reclassified from suggesting probable to indicating definite tubal ectopic pregnancy. *Ultrasound Obstet Gynecol*. 2018;51(4):543–549. doi:10.1002/uog.17435
32. Mutiso SK. Correlation of sonographic with intraoperative findings in laparoscopic managed ectopic pregnancies, a 10-year synopsis: a restrospective observational study. *BMC Pregnancy Childbirth*. 2024;24(1):296. doi:10.1186/s12884-024-06441-y
33. Yan L, Wang Y, Zhang H, et al. Deeper trophoblastic invasion and more-promotive vascular remodeling in tubal isthmic pregnancy compared with ampullary pregnancy: a retrospective clinicopathological study. *Reprod Sci*. 2025;32(5):1743–1755. doi:10.1007/s43032-025-01841-7
34. Richardson A, Gallos I, Dobson S, Campbell BK, Coomarasamy A, Raine-Fenning N. Accuracy of first-trimester ultrasound in diagnosis of tubal ectopic pregnancy in the absence of an obvious extrauterine embryo: systematic review and meta-analysis. *Ultrasound Obstet Gynecol*. 2016;47(1):28–37. doi:10.1002/uog.14844
35. Goksedef BP, Kef S, Akca A, Bayik RN, Cetin A. Risk factors for rupture in tubal ectopic pregnancy: definition of the clinical findings. *Eur J Obstet Gynecol Reprod Biol*. 2011;154(1):96–99. doi:10.1016/j.ejogrb.2010.08.016
36. Sefogah PE, Oduro NE, Swarray-Deen A, et al. Factors associated with ruptured ectopic pregnancy: a 10-year review at a district hospital in Ghana. *Obstet Gynecol Int*. 2022;2022(1491419):1–6. doi:10.1155/2022/1491419
37. Sindos M, Togia A, Sergentanis TN, et al. Ruptured ectopic pregnancy: risk factors for a life-threatening condition. *Arch Gynecol Obstet*. 2009;279(5):621–623. doi:10.1007/s00404-008-0772-7
38. Pregnancy Ewgo E, Kirk E, Ankum P, et al. Terminology for describing normally sited and ectopic pregnancies on ultrasound: ESHRE recommendations for good practice. *Hum Reprod Open*. 2020;2020(4):hoaa055. doi:10.1093/hropen/hoaa055
39. NICE. Ectopic pregnancy and miscarriage: diagnosis and initial management. *NICE guideline NG126*. 2019. Available from: https://www.nice.org.uk/guidance/ng126. Accessed September 08, 2025.
40. Verma ML, Singh U, Solanki V, Sachan R, Sankhwar PL. Spectrum of ectopic pregnancies at a tertiary care center of northern India: a retrospective cross-sectional study. *Gynecol Minim Invasive Ther*. 2022;11(1):36–40. doi:10.4103/GMIT.GMIT_1_21
41. Fleischer AC, Pennell RG, McKee MS, et al. Ectopic pregnancy: features at transvaginal sonography. *Radiology*. 1990;174(2):375–378. doi:10.1148/radiology.174.2.1688662
42. Nyberg DA, Hughes MP, Mack LA, Wang KY. Extrauterine findings of ectopic pregnancy of transvaginal US: importance of echogenic fluid. *Radiology*. 1991;178(3):823–826. doi:10.1148/radiology.178.3.1994425
43. Winder S, Reid S, Condous G. Ultrasound diagnosis of ectopic pregnancy. *Australas J Ultrasound Med*. 2011;14(2):29–33. doi:10.1002/j.2205-0140.2011.tb00192.x
44. Abrams BJ, Sukumvanich P, Seibel R, Moscati R, Jehle D. Ultrasound for the detection of intraperitoneal fluid: the role of Trendelenburg positioning. *Am J Emerg Med*. 1999;17(2):117–120. doi:10.1016/S0735-6757(99)90040-2
45. Winter TC. Ectopic pregnancy: hemoperitoneum does not equate to tubal rupture. *Radiographics*. 2021;41(1):318–320. doi:10.1148/rg.2021200199
46. Liu X, Song L, Wang J, Liu Q, Liu Y, Zhang X. Diagnostic utility of CT in differentiating between ruptured ovarian corpus luteal cyst and ruptured ectopic pregnancy with hemorrhage. *J Ovarian Res*. 2018;11(1):5. doi:10.1186/s13048-017-0374-8
47. Li PC, Lin WY, Ding DC. Risk factors and clinical characteristics associated with a ruptured ectopic pregnancy: a 19-year retrospective observational study. *Medicine*. 2022;101(24):e29514. doi:10.1097/MD.0000000000029514
48. Chong KY, de Waard L, Oza M, et al. Ectopic pregnancy. *Nat Rev Dis Primers*. 2024;10(1):94. doi:10.1038/s41572-024-00579-x
49. Yeniocak AS, Tercan C, Dagdeviren E, Arabaci O, Genc EE. Evaluation of a scoring system to predict treatment success with single-dose methotrexate in ectopic pregnancy. *Arch Gynecol Obstet*. 2024;309(5):2047–2055. doi:10.1007/s00404-024-07458-6